

## IDENTIFYING A NON-PERMEABLE FRACTURE FOR CONVECTION AND DIFFUSION USING X-RAY COMPUTED TOMOGRAPHY

A. Polak, The Hebrew University  
A. S. Grader, The Pennsylvania State University  
R. Kehl, Kehlco, Inc., Scientific Visualization Systems

This abstract outlines an experimental method for determining whether or not a natural fracture is permeable for convective and diffusive transport processes. The evaluation was done in an effort to characterize a fractured chalk formation in the northern Negev desert in Israel that has been subjected to chemical contamination. The formation has large fractures that are very conductive and fine fractures that may be sealed. The presence of these two types of fractures creates a complicated flow system that needs to be understood prior to implementation of remediation programs.

**The core:** The core was retrieved from a depth of 18.3 m in a deviated well. The core was about 20 cm long with a diameter of 5 cm, with an estimated absolute air permeability of about 0.4 mD and a porosity of 33%. About 80% of the core was calcite. The sample contained a thin natural fracture that was visible to the naked eye. This fracture was diagonal to the long axis of the core, close to one end. The core was artificially fractured using a modified Brazilian test that included longitudinal cleaving. **Figure 1** shows a photograph of the sample with the natural fracture and **Figure 2** shows the sample after it was broken in two parts. The presence of the natural fracture is evident in **Figure 2**, and the artificial fracture followed the natural fracture in the region where they intersected for distance of about 1 cm.

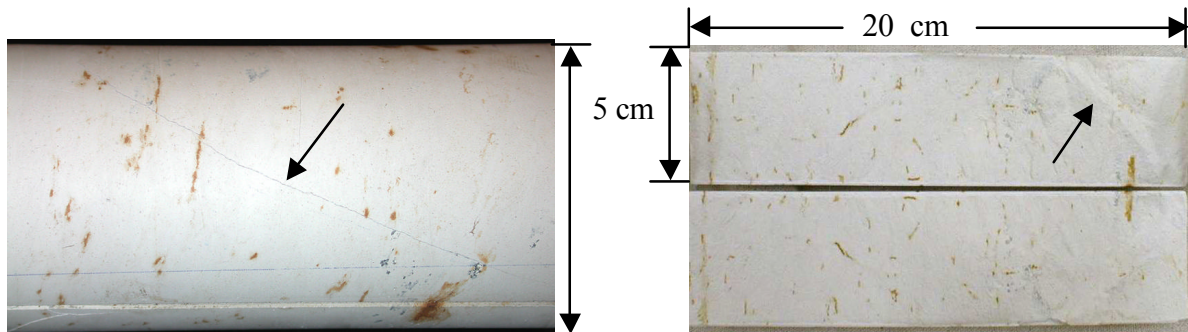


Figure 1: A photograph of the core showing the natural fracture denoted by the arrow.

Figure 2: A photograph of the fractured core in book format. The natural fracture is denoted by the arrow.

**Experimental Procedure:** The core was assembled into a bi-axial core holder shown in **Figure 3**. Some chalk spacers were placed between the two parts of the core to ensure that the fracture remained open with an estimated gap of between 0.5 and 1.0 mm. At both ends of the sample gaskets were placed with slits that matched exactly the end locations of the fracture. This assembly permits the injection of water and tracer only into the fracture, and reduces convective flow in the matrix. After the core was loaded into the core holder, a confining pressure of about 300 psig was applied

and the core assembly was placed inside an x-ray fourth generation medical scanner. The images that were obtained had a thickness of 2 mm, with an in-plane pixel resolution of about 0.3 - 0.5 mm. The movements of fluids in the core were measured by X-ray computed tomography and visualized as a function of space and time. A vacuum was created in the core followed by the introduction of non-tagged water. During the process of water invasion, images were collected and used to determine the convective properties of the natural fracture. After the sample was saturated, water tagged with NaI (5% by weight) was continuously injected into the fracture, fixing the diffusion boundary condition. The diffusion process was monitored by the CT scanner, allowing us to determine the response of the fracture.

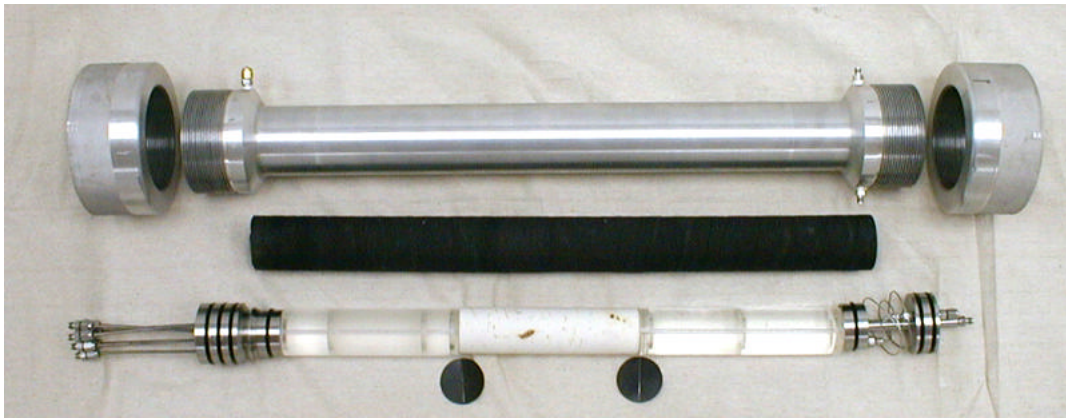


Figure 3: A photograph of the entire core holder assembly.

A typical single CT slice through the sample is shown in **Figure 4a** and a longitudinal reconstruction through the center of the sample is shown in **Figure 4b**. The figure shows the natural fracture and the artificial fracture. Injection is from left to right.

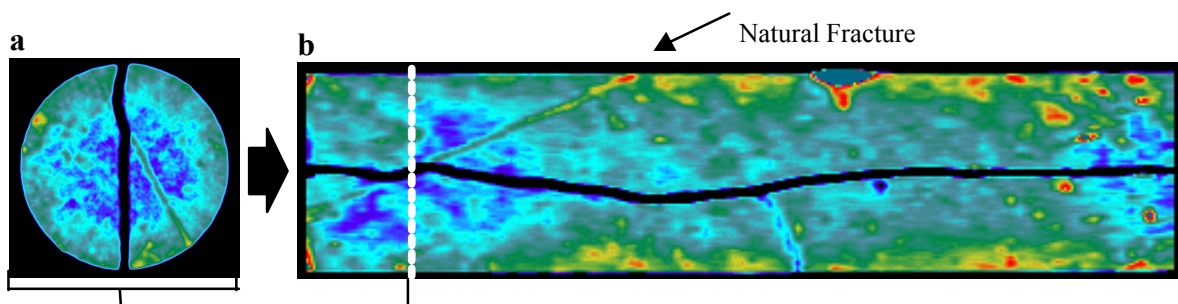


Figure 4: An example of a single CT image and a central horizontal reconstruction.

**Convection:** During the water invasion period, images were taken along the sample. **Figure 5** shows a series of scans taken at one position during the invasion of water. The images are presented in a gray scale that is divided into 10 levels, hence providing a combination gray color map as well as a contour map. The water fills up the fracture and then starts invading the low permeability matrix. The image at the left side was taken just after the water invasion process began. The light color on both sides of the fracture denotes the invasion of water. The following four images were taken at 6, 9, 18, and 63 minutes after the start of water flow. The natural fracture that appears mainly on the right side of the figure in a diagonal mode from upper left to

lower right did not allow water to flow across it. It is clearly seen in the three right images in **Figure 5**. The water entered the region to the right of the natural fracture from the top, the point where the natural fracture is intersected by the artificially-created fracture. The upper set of images show the actual scan data. The natural fracture appears with high CT values before it was surrounded by water indicating that it may be less porous or may be a high density material. The lower set of images show the net presence of water by subtracting the dry scans from the wet scans at the same positions taken during the water invasion stage. The lower set of images shows that the fracture is sealed to the flow of water. It also shows the steady progression of water into the matrix on the left side of the core. **Figure 6A** shows the net presence of water as a function of time along the center of the sample as shown in the inset image. The profiles demonstrate that the natural fracture is preventing water from crossing it. The natural fracture is most likely calcite-filled.

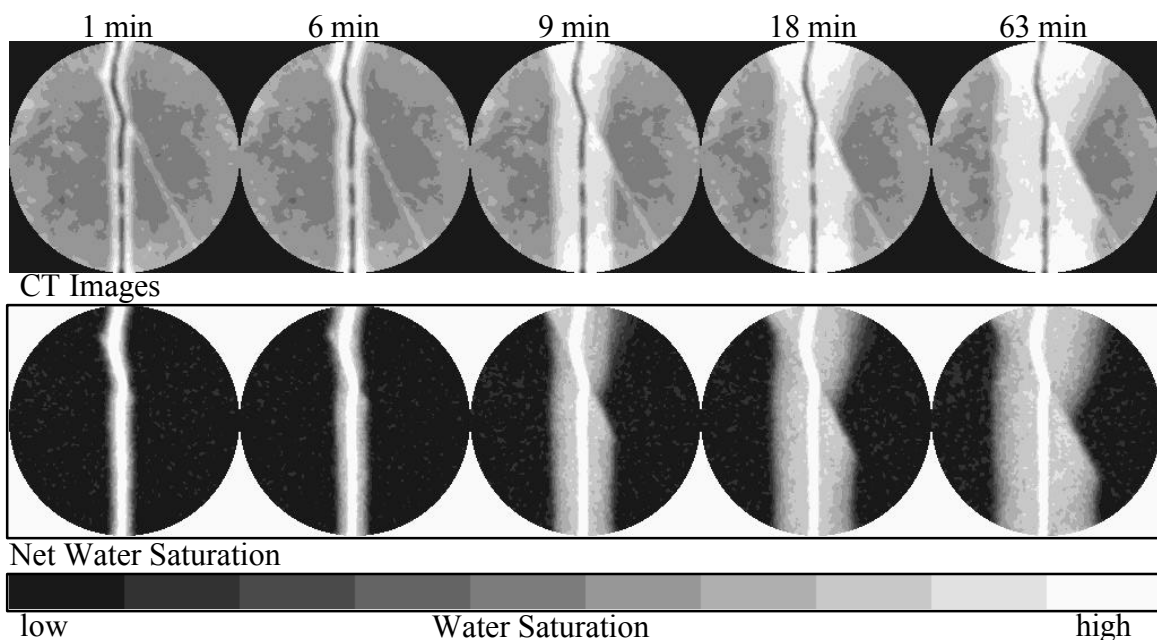


Figure 5: Five images showing the invasion of water into the core. The natural fracture formed a barrier to convective flow of water, shown to the right of the images. Top set: CT images. Bottom set: CT values of net water obtained by image subtraction.

**Diffusion:** After the core was fully saturated with water (without tracer) a final CT scanning sequence was done to cover the entire sample. Then, water with 5% NaI by weight as a tracer was continuously injected into the fracture. The continuous injection changed the NaI concentration in the fracture to a constant and provided a fixed boundary condition for diffusion of NaI from the fracture into the matrix. We followed the same position as shown in Figure 5 and also acquired CT data along the entire length of the core. The main goal of the experiment was to collect temporal and spatial concentration data during forward and backward diffusion processes so that diffusion coefficients can be determined. However, this abstract focuses only on the

initial forward diffusion period in order to determine whether the fracture formed a barrier to diffusion.

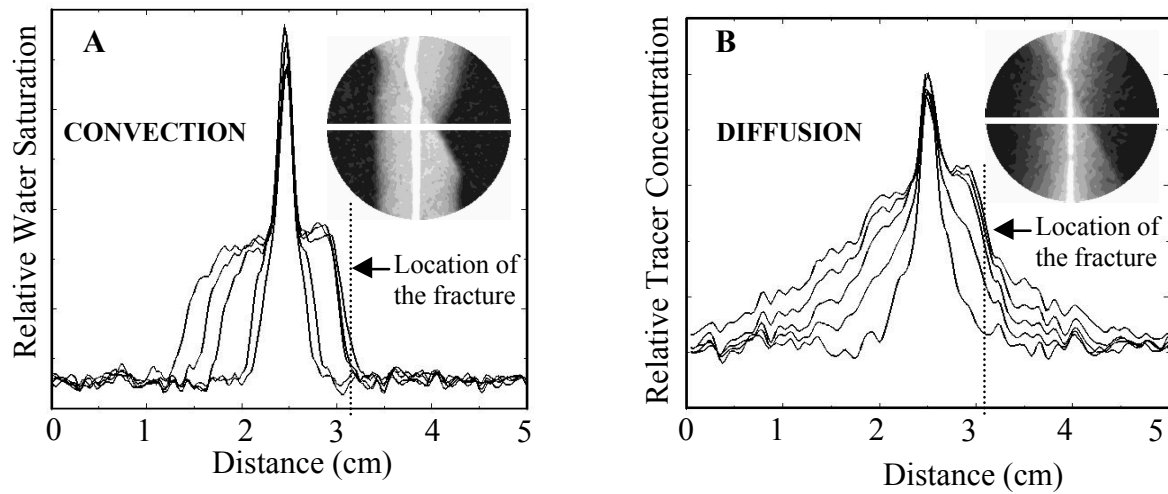


Figure 6: **A:** Water saturation profiles in the center of the sample. **B:** Iodine concentration profiles in the center of the sample.

During the steady flow of tagged water through the fracture, iodine diffused into the high porosity and low permeability matrix. The progression of the diffusion process in the same location shown during convection is presented in **Figures 6B** and **7**. The figure demonstrates that the natural fracture did not permit diffusion across it during the time scale of the experiment. The relative concentration of the tracer at any position in the core was computed, but not discussed in this abstract due to lack of space. However, the conversion of the images to true concentration images must include three-dimensional porosity maps, that were obtained after the water saturation stage. The abstract highlights the visualization and quantification aspects of CT imaging in capturing four-dimensional fluid flow processes such as convection and diffusion.

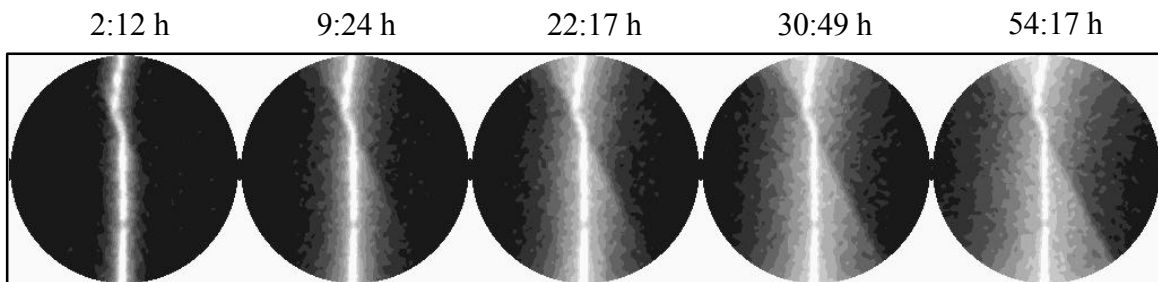


Figure 7: Five images showing the diffusion of tracer in the core. The natural fracture formed a barrier to diffusion shown to the right of the images.